

Dynamic second-order hyperpolarizabilities of Si₂C and Si₃C clusters using coupled cluster singles-and-doubles response approach

You-Zhao Lan*¹, Yun-Long Feng

Zhejiang Key Laboratory for Reactive Chemistry on Solid Surfaces, Institute of Physical Chemistry, Zhejiang Normal University, Zhejiang, Jinhua 321004, China

Abstract

We investigate the dynamic second-order hyperpolarizabilities $\gamma(-3\omega; \omega, \omega, \omega)$ (indicated by γ^{THG}) of the Si₂C and Si₃C clusters using highly accurate coupled cluster singles-and-doubles (CCSD) response approach. The static γ values of the Si₂C and Si₃C clusters are 1.99×10^{-35} and 3.16×10^{-35} esu, respectively. The dynamic γ values of the Si₂C and Si₃C clusters have wide non-resonant optical region. Similar to the α , the $\gamma_{||}$ value of the Si₂C cluster is smaller than that of the Si₃ cluster, which is most likely related to much smaller static $\gamma_{||}$ value of the C atom than the Si atom because these two clusters have a similar geometry (or shape). Similar reason is for smaller γ values of the Si₃C cluster than the Si₄ cluster. Several Si₂C isomers with C_{2v} symmetry, which are obtained by using potential energy surface scan (PESS) calculations, have the same bond length of Si–C and different bond angles of Si–C–Si. The $\gamma_{||}$ values of the Si₂C isomers increase with an increase of the bond angle of Si–C–Si. This angle-dependence can be related to a change of the highest occupied molecular orbitals (HOMO) from σ -electron to π -electron framework and no change for the lowest unoccupied molecular orbitals (LUMO). A change of HOMO is ultimately attributed to alternative sp² and sp hybridizations of the C atom.

1. Introduction

The (hyper)polarizabilities of small semiconductor clusters, such as gallium arsenide (GaAs), silicon (Si), and silicon carbide (SiC) clusters, have attracted much attention in the past 20 years¹⁻²¹. The optical properties of small semiconductor clusters exhibit markedly different features from those of their corresponding bulk materials. Clusters²² may be optically active even though the bulk material is not active because clusters have a different energy band structure from bulk

¹ Corresponding author: Youzhao Lan; Postal address: Zhejiang Key Laboratory for Reactive Chemistry on Solid Surfaces, Institute of Physical Chemistry, Zhejiang Normal University, Jinhua 321004, China; Fax: +086 579 82282269; E-mail address: lyzhao@zjnu.cn

materials and more localized intermediate states than the bulk; moreover, there are some localized states in clusters but not in bulk.

Numerous researches have contributed to the isotropic dipole polarizabilities α of the Si and GaAs clusters^{1-10,12,16,21}. For small Si_n ($n < 10$) and Ga_nAs_m ($n + m < 8$) clusters, the α values are greater than the bulk value and decrease with increasing the cluster size^{1,2,9,12,16}; moreover the α values of these small clusters depend directly on the cluster size and indirectly on the HOMO–LUMO energy gap⁸. For mediate-size Si_n ($n = 9 - 50$) and Ga_nAs_m ($n + m = 9 - 30$) clusters, experimental α values¹² vary strongly and irregularly with cluster size and fluctuate around the bulk value. For large Si_n ($n = 60 - 120$), all experimental α values are smaller than the bulk value¹². However, for the Si_n ($n = 9 - 28$) clusters, Deng *et al.*⁶ found that theoretical α values exhibit fairly irregular variations with the cluster size and all calculated values are higher than the bulk value. Similar theoretical results have been also obtained by Sieck *et al.*²¹ and Jackson *et al.*⁷ for the Si_n ($n = 1, 3 - 14, 20, \text{ and } 21$) and ($n = 1 - 21$) clusters, respectively. Therefore, for intermediate-size Si_n ($n = 9 - 28$), some discrepancies exist between experimental and theoretical static α values and more investigations are needed. Besides an interesting size-dependence of the α values, a shape-dependence has been also theoretically reported by Jackson *et al.*⁴ for the Si_n ($n = 20 - 28$) clusters. Our recent theoretical study showed that the α values of the SiC_n and Si_nC ($n = 2 - 6$) clusters are larger than the bulk polarizability of 3C-SiC and lie between the dipole polarizabilities of the Si and C atoms¹⁵.

For the first- and second-order hyperpolarizabilities (β and γ), a few studies have been performed on the Si_n ($n = 3 - 8$ and 10) [Ref. 13 and 20], Ga_mAs_n ($m + n = 4 - 10$) [Ref. 17 and 19], Ga_nAs_n ($n = 2 - 9$) [Ref. 23], and Si_nC and SiC_n ($n = 2 - 6$) [Ref. 15]. The β , which strongly depends on the symmetry of the cluster, is vanish for many clusters, such as Si_4 and Ga_2As_2 clusters with D_{2h} symmetry^{17,20}. The macroscopic nonlinear polarizabilities ($\chi^{(2)}$ and $\chi^{(3)}$) of small Ga_mAs_n ($m + n = 5 - 10$) clusters based on the sum-over-states (SOS) calculations and local-field corrections are close to the bulk value¹⁷. For small Ga_nAs_n clusters up to ten atoms, the γ values are in the range of $1.5 \times 10^5 - 3.2 \times 10^5$ a.u. obtained using *ab initio* finite field at second order Møller-Plesset perturbation theory (MP2) level²³. Silicon nanoclusters were experimentally expected to have strong and large third-order optical nonlinearity $\chi^{(3)}$ and their optical properties are strongly correlated with the size of the clusters^{24,25}. *ab initio* finite field calculations were also

carried out on the static γ values of small Si_n ($n = 3 - 8$) clusters²⁰ and showed that clusters with even atom number increase the γ value in the size-dependence of the γ values, while ones with odd atom number decrease the γ value. The best theoretic static γ values of the Si_3 and Si_4 clusters are about 5×10^{-35} esu based on highly accurate coupled cluster (CC) calculations^{10,14}. For the Si_nC and SiC_n ($n = 2 - 6$) clusters, the C-rich clusters have lower α and larger β than the Si-rich clusters¹⁵. The size-dependence of the β values of the SiC_n ($n = 2 - 6$) clusters, which have approximate Si-terminated linear chain geometry, is similar to that observed in π -conjugated organic molecules.

The above mentioned experimental and theoretical studies show that investigating the (hyper)polarizabilities of semiconductor clusters are all along a topic of interest. The magnitude of nonlinear polarizabilities depend primarily on the symmetry of the cluster and prove to be high for the low-symmetry clusters¹³. Small SiC clusters exhibit similar α and β to the Si and GaAs clusters. These semiconductor clusters are expected to have potential applications in the nonlinear optical nano-materials engineering. Little is known, however, about the γ of the SiC material. More recently, the coupled perturbed Hartree Fock (CPHF) calculations²⁶ for periodic system showed that the magnitude of $\chi_{ijij}^{(3)}$ ($i, j = x, y, z$) is of the order of 10^{-14} esu for cubic SiC bulk (experimental lattice parameter: 4.358 Å). In this paper, we investigate the static and dynamic γ of the Si_2C and Si_3C clusters. A highly accurate calculation method, the response theory within *ab initio* CCSD framework, is employed.

In Section 2, we provide the theory and computational details. In Section 3, we give the basis set dependence of $\gamma(0)$ values, the dynamic γ^{THG} of the Si_2C and Si_3C clusters, a comparison with the γ^{THG} of the Si_3 and Si_4 clusters, and the γ^{THG} of the Si_2C isomers. Finally, we summarize our results in Section 4.

2. Theory and Computational Details

Most stable geometries of the Si_2C and Si_3C clusters were obtained from the literature²⁷⁻³¹ and reoptimized at the DFT/aug-cc-pVTZ level using the Gaussian 03 program³² with the hybrid Becke3-Lee-Yang-Parr (B3LYP) functional. The vibrational frequencies were calculated to confirm that the final geometries are stable without an imaginary frequency. The final geometries and symmetries of the Si_2C and Si_3C clusters are shown in Fig. 1.

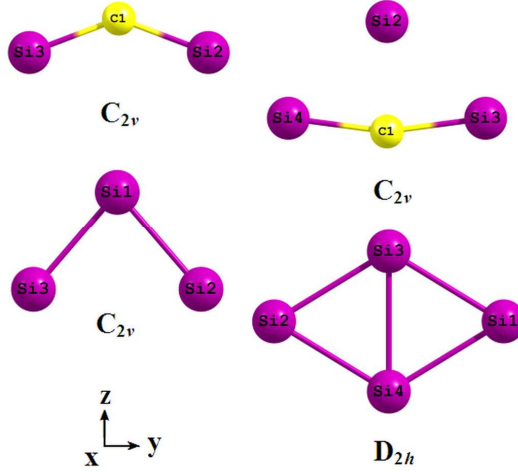


Figure 1. Geometries of the Si_2C , Si_3C , Si_3 , and Si_4 clusters.

To calculate the γ , we used the CCSD response approach, as implemented in the Dalton 2.0 program³³. According to the response theory³⁴, the expectation value of the time-dependent operator A , which corresponds to one of the properties of these molecular systems, can be expressed in terms of the response functions,

$$\begin{aligned}
\langle t | \hat{A} | t \rangle &= \langle 0 | \hat{A} | 0 \rangle \\
&+ \int \langle \langle \hat{A}; \hat{B}^{\omega_1} \rangle \rangle_{\omega_1} \times \exp(-i\omega_1 t) d\omega_1 \\
&+ \frac{1}{2} \iint \langle \langle \hat{A}; \hat{B}^{\omega_1}, \hat{C}^{\omega_2} \rangle \rangle_{\omega_1, \omega_2} \times \exp[-i(\omega_1 + \omega_2)t] d\omega_1 d\omega_2 \\
&+ \frac{1}{6} \iiint \langle \langle \hat{A}; \hat{B}^{\omega_1}, \hat{C}^{\omega_2}, \hat{D}^{\omega_3} \rangle \rangle_{\omega_1, \omega_2, \omega_3} \times \exp[-i(\omega_1 + \omega_2 + \omega_3)t] d\omega_1 d\omega_2 d\omega_3 \\
&+ \dots
\end{aligned}$$

where $\langle 0 | \hat{A} | 0 \rangle$ is the expectation value of A in the absence of internal or external perturbations; ω_1 , ω_2 , and ω_3 indicate the applied field frequencies.

$$\langle \langle \hat{A}; \hat{B}^{\omega_1} \rangle \rangle_{\omega_1}, \quad \langle \langle \hat{A}; \hat{B}^{\omega_1}, \hat{C}^{\omega_2} \rangle \rangle_{\omega_1, \omega_2} \quad \text{and} \quad \langle \langle \hat{A}; \hat{B}^{\omega_1}, \hat{C}^{\omega_2}, \hat{D}^{\omega_3} \rangle \rangle_{\omega_1, \omega_2, \omega_3}$$

denote the linear, quadratic, and cubic response functions, respectively. When A , B , C , and D denote the components of the electric dipole operator, these three response functions are the negative values of the dipole polarizability, first-order hyperpolarizability, and second-order hyperpolarizability, namely, $-\alpha(-\omega_1; \omega_1)$, $-\beta(-\omega_1-\omega_2; \omega_1, \omega_2)$, and $-\gamma(-\omega_1-\omega_2-\omega_3; \omega_1, \omega_2, \omega_3)$, respectively. Response expressions for calculating the frequency-dependent (*i.e.*, dynamic) (hyper)polarizabilities have been derived and implemented within the framework of both the *ab-initio* theory³⁵⁻³⁷ and the density functional theory^{38, 39}. For the *ab-initio* theory, the coupled cluster cubic response theory systematically improves the positions of the poles in the response

functions and considers the dynamical electron correlation effects, which are very important for determining the dynamic hyperpolarizabilities. A detailed description of the coupled cluster cubic response theory used to calculate the γ can be obtained from Ref. 37.

To obtain accurate γ , we mainly consider the choice of both coupled cluster models and basis sets. The inclusion of double excitation in the coupled cluster theory is proved to be important for the hyperpolarizability^{36,37}. In this study, we employ the CCSD response approach to calculate the dynamic hyperpolarizabilities γ for the third-harmonic generation (THG) technique. In the usual experiments, two components, γ_{\parallel} and γ_{\perp} , are measured⁴⁰, where the optical field is polarized parallel and perpendicular to the static field, respectively. We focus on the scalar component of the tensor γ , which is defined by the isotropic average, $\gamma_{\parallel} = (1/15) \sum_{ij} (\gamma_{iij} + \gamma_{ijj} + \gamma_{jij})$, where $i, j = x, y, z$. In the static limit, γ_{\parallel} is equal to the static isotropic average $\langle \gamma \rangle = (1/5) \sum_{ij} \gamma_{iij}(0)$. For ease of choice of the basis sets, we provide the basis set dependence of $\gamma_{\parallel}(0)$ in Subsection 3.1 and select the d-aug-cc-pVDZ basis set, which has reached the basis set limit, for calculating the dynamic γ .

3. Results and Discussion

3.1. Basis set dependence of $\gamma_{\parallel}(0)$

Both the electron correlation effects and the quality of the basis set are important for the hyperpolarizability calculations³⁶⁻⁴¹. The coupled cluster theory can efficiently deal with the dynamical correlation effects.^{36,37,42,43} Here, we only perform the CCSD calculations because the CCSD model has been also proved to give accurate values for the optical properties based on the cubic response function, such as second-order hyperpolarizability and two-photon transition strength^{37,42,43}. For the choice of the basis set, sufficient polarization and diffuse functions generally need to be involved in the basis set^{14,37,44}. Both the Pople basis sets and the Dunning basis sets that include no diffuse functions (*e.g.*, 6-31G, 6-311G, 6-311G*, cc-pVDZ, and cc-pVTZ) would result in an irregularity in the sign or the value of γ (Ref. 14). To obtain accurate γ , at least one set of diffuse basis functions should be added in the basis set. Similar case occurs in the CCSD calculations of the two-photon absorption property⁴⁵ that is related to the cubic response function. Paterson *et al.*⁴² showed that the unaugmented Dunning basis sets gives about one order of magnitude smaller two-photon transition strength (δ^{TPA}) than the augmented ones. For example,

in the CCSD calculations, the cc-pVDZ and aug-cc-pVDZ basis sets give the δ^{TPA} values of 0.025 and 0.187 a.u. for the formaldehyde (CH₂O) molecule, respectively. They also showed that the coupled cluster δ^{TPA} values based on the Pople basis sets are very poor and suggested that the Pople basis sets should be avoided in two-photon coupled cluster calculations. In our recent work ¹⁴, the Dunning basis set is also proved to be more suitable for the hyperpolarizability calculations than the Pople basis set.

Therefore, to estimate the basis set dependence of γ , we used the Dunning basis sets to calculate the $\gamma_{\parallel}(0)$ values of the Si₂C and Si₃C clusters. The calculated results are collected in Table 1. For comparison, we also provided the $\gamma_{\parallel}(0)$ obtained using the HF response calculations in Table 1. As expected, the unaugmented Dunning basis sets give erratic $\gamma_{\parallel}(0)$ values for both the CCSD and the HF response approaches. Addition of one set of diffuse functions significantly improves the results (see aug-cc-pVXZ: X = D and T). For the singly augmented basis sets, increasing the cardinality results in an increase of the $\gamma_{\parallel}(0)$ value (also see aug-cc-pVXZ: X = D and T). However, for both the doubly and the triply augmented basis sets, increasing the cardinality results in a slight decrease of the $\gamma_{\parallel}(0)$ value (see x-aug-cc-pVXZ: x = d and t, X = D and T). The $\gamma_{\parallel}(0)$ values based on the doubly augmented basis set appear to reach the basis set limit. In the CCSD calculations of δ^{TPA} , Paterson *et al.* ⁴² showed that the δ^{TPA} values reach the basis set limit in the augmented triple-zeta basis sets and the singly and doubly augmented basis sets give very close δ^{TPA} values beyond the triple-zeta level. Further, for the HF response approach, which does not deal with the electron correlation, the HF $\gamma_{\parallel}(0)$ values are smaller than the CCSD ones by an error of between 8% and 18%. On the basis of Paterson *et al.*'s work ⁴² and our present results, we select the d-aug-cc-pVDZ basis set for calculating the excited state properties and dynamic hyperpolarizabilities in order to reduce the computational costs and also owing to the non-availability of experimental results for the direct comparison for the Si₂C and Si₃C clusters.

Table 1. Basis set dependence of $\gamma(0)$ ($\times 10^{-35}$ esu) of the Si_2C and Si_3C clusters obtained using the CCSD and HF response calculations. ($1 \text{ au} = 6.235 \times 10^{-65} \text{ C}^4 \text{ m}^4 \text{ J}^{-3} = 5.036 \times 10^{-40} \text{ esu}$)

$\gamma(0)$	CCSD		HF		Error ^a	
	Si_2C	Si_3C	Si_2C	Si_3C	Si_2C	Si_3C
cc-pVDZ	-0.300	-0.056	-0.079	0.001		
cc-pVTZ	-0.060	0.270	0.074	0.274		
aug-cc-pVDZ	1.607	2.674	1.316	2.212	0.18	0.17
aug-cc-pVTZ	1.788	2.802	1.558	2.549	0.13	0.09
d-aug-cc-pVDZ	1.992	3.157	1.636	2.670	0.18	0.15
d-aug-cc-pVTZ	1.955	2.952	1.724	2.707	0.12	0.08
t-aug-cc-pVDZ	2.014	3.160	1.661	2.675	0.18	0.15
t-aug-cc-pVTZ	1.961	2.963	1.730	2.719	0.12	0.08

$$^a \text{Error} = (\text{CCSD} - \text{HF})/\text{CCSD}$$

3.2. Dynamic second-order hyperpolarizabilities: $\gamma_{||}^{\text{THG}}$

Before the $\gamma_{||}^{\text{THG}}$, we investigate the absorption spectra of the Si_2C and Si_3C clusters. The absorption spectrum can provide important information on one- or multi-photon resonant absorption. One-photon or multi-photon absorption resonance enhancements will possibly lead to an irregularity in the sign and numerical value of the calculated hyperpolarizabilities and higher optical damage that should be avoided in nonlinear optical experiments^{14, 41}. Although the absorption spectra of the Si_2C and Si_3C clusters have been calculated using the linear response density functional theory (LRDFT) at the B3LYP/aug-cc-pVTZ level¹⁵, the coupled cluster based methods will possibly improve the excitation energies and oscillator strengths^{36, 37, 42}. To obtain the CCSD absorption spectra, we calculated the excitation energies and oscillator strengths of the Si_2C and Si_3C clusters using the CCSD/d-aug-cc-pVDZ response calculations. Calculations were performed using the Dalton 2.0 program³³. Then, we fitted the obtained excitation energies and oscillator strengths to the absorption spectra using Gabedit program⁴⁶ and a Lorentzian model with a half-bandwidth of 0.05 eV was used.

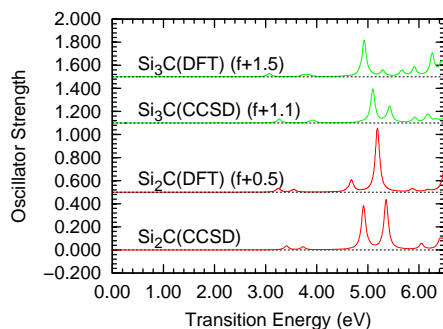


Figure 2. Absorption spectra of the Si_2C and Si_3C clusters based on the CCSD/d-aug-cc-pVDZ and the B3LYP/aug-cc-pVTZ [Ref. 15] response calculations. Note that 0.5, 1.1, or 1.5 has been added to the oscillator strengths (f) to clearly display the plots.

Figure 2 shows the absorption spectra of the Si_2C and Si_3C clusters, where the transition energy (TE) is less than 6.5 eV. For convenience of comparison, the calculated LRDFFT absorption spectra¹⁵ are also included in Fig. 2. The CCSD absorption spectra of the Si_2C and Si_3C clusters exhibit common characteristics of small semiconductor clusters with the number of atoms less than 10, such as Si_n ($n = 3 - 10$) [Ref. 16 and 14] and Ga_nAs_m ($n + m \leq 10$) [Ref. 17, 18, and 47] clusters, that is, long absorption tails exist in the low-TE (<4.5 eV) region and strong allowed absorption peaks are located in the high-TE (>4.5 eV) region. In Fig. 2, the CCSD spectra are similar to the LRDFFT spectra in terms of the peak positions and their envelopes except that the former exhibits a blue-shift (~ 0.1 eV). For clarity, Table 2 lists the transition energies (oscillator strengths) of the first excited state and the first strong allowed transition state for the Si_2C and Si_3C clusters. Note that the coupled cluster response theory has been shown to give highly accurate results for the excitation energies and oscillator strength^{48, 49}. For the augmented Dunning basis sets (e.g. x-aug-cc-pVXZ: x = s, d, and t, X = D and T), the excitation energies based on different coupled cluster models (e.g. CCS, CC2, and CCSD) or different hybrid density functionals (e.g. B3LYP, BPW91, and B3P86) are very close^{15, 42}. For instance, for the lowest excited state of the CH_2O molecule, Paterson *et al.*⁴² showed that the exact energies based on the CCSD response calculations with the aug-cc-pVDZ, d-aug-cc-pVDZ, and t-aug-cc-pVDZ basis sets are 4.006, 3.998, and 3.997 eV, respectively. Therefore, our present CCSD/d-aug-cc-pVDZ results can provide the reliable linear absorption properties.

Table 2. Transition energies (eV) and oscillator strengths (in parenthesis) of the first excited state and the first strong allowed transition for the Si₂C and Si₃C clusters.

Cluster	First excited state		First strong allowed transition state	
	CCSD	LRDFT	CCSD	LRDFT
Si ₂ C	3.19 (0.0)	3.08 (0.0)	4.92 (0.3754)	4.68 (0.0998)
Si ₃ C	2.02 (0.0017)	1.87 (0.0015)	5.10 (0.2912)	4.93 (0.3112)

On the basis of the CCSD absorption spectra, we find that the Si₂C and Si₃C clusters have no obvious linear absorption in the region (< 4.5 eV) and have wide transparent region (< 3.0 eV). Therefore, we focus on the dynamic $\gamma_{\parallel}^{\text{THG}}$ of the Si₂C and Si₃C clusters with the applied field energies less than 2.0 eV. Figure 3 shows the dynamic γ obtained using the CCSD/d-aug-cc-pVDZ response calculations. The three main components of the tensor γ (γ_{xxxx} , γ_{yyyy} , and γ_{zzzz}) and the average $\gamma_{\parallel}^{\text{THG}}$ are provided, and the molecular orientations are shown in Fig. 1. Resonance enhancements at $\hbar\omega = 1.63$ eV (0.06 a.u.) are clearly observed for the Si₂C and Si₃C clusters. In the THG process, resonance enhancements will possibly occur at $\hbar\omega$, $2\hbar\omega$, and $3\hbar\omega$ applied field energies. A resonance results in a dispersion in the γ values. For the Si₂C cluster, a resonance enhancement at 1.63 eV possibly is related to the $2\hbar\omega$ or the $3\hbar\omega$ resonance because the (1.63 eV $\times 2$) and (1.63 eV $\times 3$) are close to the transition energies of the first excited state (3.19 eV) and the first strong allowed transition state (4.92 eV) (Table 2), respectively. However, the oscillator strength of the first excited state is 0.0; thus the $2\hbar\omega$ resonance can be ignored. For the $3\hbar\omega$ resonance, we can see from Table 2 that there would be an actual absorption of photons because the oscillator strength (f) for the excited state of 4.92 eV is 0.3754. Similarly, for the Si₃C cluster, a resonance enhancement at 1.63 eV is related to the $3\hbar\omega$ resonance on the basis of the excited state of 5.10 eV (Table 2). The commonly employed laser wavelengths of 1064 (1.16) and 1907 nm (0.65 eV) are significantly different from the first strong resonance absorption energies at which the optical damage and thermal effects possibly occur; thus, the Si₂C and Si₃C clusters, as well as the Si₃ and Si₄ clusters¹⁴, are potential candidates for THG nonlinear optical materials in the infrared range.

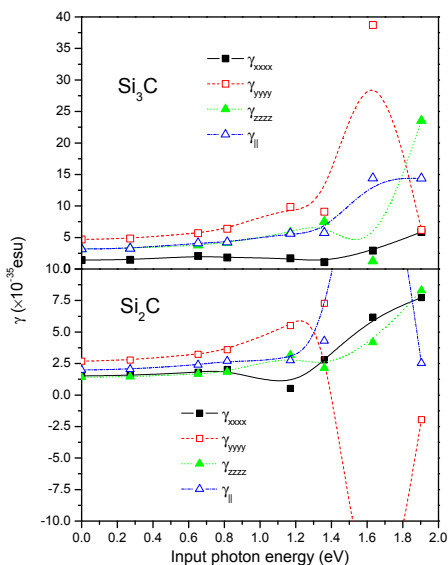


Figure 3. Dynamic second-order hyperpolarizabilities γ of the Si_2C and Si_3C clusters based on the CCSD/d-aug-cc-pVDZ response calculations. ($1 \text{ au} = 6.235 \times 10^{-65} \text{ C}^4 \text{ m}^4 \text{ J}^{-3} = 5.036 \times 10^{-40} \text{ esu}$). For clarity, for the Si_2C cluster, two data points ($\gamma_{||}$ and γ_{yyyy} at 1.63 eV) are not shown, and they are 28.74×10^{-35} and -24.72×10^{-35} esu, respectively.

3.3. Comparison with the $\gamma_{||}^{\text{THG}}$ of the Si_3 and Si_4 clusters

As shown in Fig. 1, geometries of the Si_3 and Si_4 clusters are very similar to those of the Si_2C and Si_3C clusters. Actually, the Si_2C and Si_3C clusters can be obtained by substituting a silicon atom of the corresponding Si_3 and Si_4 clusters cluster by a carbon atom. The obtained geometries of the Si_2C and Si_3C clusters by direct substitution would be unstable, and then relax to stable geometries. Researches on the static α have shown that the static α values of the Si_3 and Si_4 clusters are around 5.15 and 5.10 $\text{\AA}^3/\text{atom}$ based on different calculation methods ^{1,2,8,9,16}, respectively, and that the static α values of the Si_2C and Si_3C clusters are 4.04 and 4.00 $\text{\AA}^3/\text{atom}$ based on the LRDFFT calculations ¹⁵, respectively. It has been shown that the size of the α value is possibly related to the shape of the cluster or the energy difference between the molecular orbital levels. For example, for the Si_n ($n = 3 - 10$) clusters, Pouchan *et al.* ⁸ showed that more prolate structures are more polarizable and the α value is directly related to the size of the energy gap between symmetry-compatible bonding and antibonding molecular orbitals. Jackson *et al.* ⁴ also found a clear shape-dependence for the calculated α values of the Si_n ($n = 20-80$) clusters and

clusters with prolate structures have systematically larger polarizabilities than those with compact structures. The reason why the static α value of the Si₂C cluster is smaller than that of the Si₃ cluster is most likely much smaller static α value of the C atom than the Si atom because the Si₂C cluster has a similar geometry (or shape) to the Si₃C cluster. Researches have shown that the C atom with a static α value of 1.88 Å³/atom [Ref. 50] is softer than the Si atom with that of ~5.54 Å³/atom [Ref. 3]. Similar reason is for the Si₃C and Si₄ cluster.

Motivated by the α , we make a comparison of the $\gamma_{||}^{\text{THG}}$ between the Si₂C and Si₃C clusters and the Si₃ and Si₄ clusters. A detailed study based on the CCSD response calculations for the $\gamma_{||}^{\text{THG}}$ values of the Si₃ and Si₄ clusters can be found in our previous work ¹⁴. Finite field calculations for the static $\gamma_{||}$ of the Si₃ and Si₄ clusters can be found in the literature ^{10, 20}. Stable geometries of the Si₃ and Si₄ clusters are also shown in Fig. 1 based on the same optimization method as for the Si₂C and Si₃C clusters. In our previous work ¹⁴, the dynamic $\gamma_{||}^{\text{THG}}$ values are based on the CCSD/aug-cc-pVTZ response calculations. For a direct comparison, we recalculated the $\gamma_{||}^{\text{THG}}$ values of the Si₃ and Si₄ clusters using the CCSD/d-aug-cc-pVDZ response calculations. The obtained results for the dynamic $\gamma_{||}^{\text{THG}}$ values are provided for $\omega = 0.0$ (∞) and 0.65 eV (1907 nm) in Table 3. Further, nine main components of the tensor γ (i.e., γ_{ijj} , $i, j = x, y, z$) are provided along with the average $\gamma_{||}^{\text{THG}}$ values. For the Si₃ cluster, Champagne *et al.* ²⁰ have used the finite field calculations of the RHF, MP2, MP3, MP4(DQ), MP4(SDQ), MP4(SDTQ), CCSD, and CCSD(T) with the 6-311+G* basis set to obtain the $\gamma_{||}(0)$ values of 2.48, 3.05, 2.76, 2.61, 2.72, 3.15, 2.74, and 3.03 ($\times 10^{-35}$) esu, respectively. In the case of the Si₄ cluster, they are 3.37, 4.52, 3.97, 4.00, 4.03, 4.42, 4.11, and 4.43 ($\times 10^{-35}$) esu, respectively. Moreover, Maroulis and Pouchan ¹⁰ obtained a $\gamma_{||}(0)$ value of 5.35×10^{-35} esu by using the finite field calculations at the CCSD(T) level with a self-designed basis sets. Combining with our present results, we can find that the Si₃ and Si₄ clusters individually have a larger $\gamma_{||}(0)$ value than the Si₂C and Si₃C clusters. In the dynamic case, the $\gamma_{||}$ values at 0.65 eV in Table 3 exhibit the same size relationship as the static $\gamma_{||}$ values, i.e., $\gamma_{||}^{\text{THG}}(\text{Si}_3) > \gamma_{||}^{\text{THG}}(\text{Si}_2\text{C})$ and $\gamma_{||}^{\text{THG}}(\text{Si}_4) > \gamma_{||}^{\text{THG}}(\text{Si}_3\text{C})$. Actually, the dynamic $\gamma_{||}$ of the Si₂C, Si₃C, Si₃, and Si₄ clusters exhibit wide non-resonant optical region (Fig. 3 in this work and Fig. 2 in Ref. 14) because their line absorption spectra have similar long absorption tails (<4.5 eV) (Fig. 2 in this work and Fig. 1 in Ref. 14). In the non-resonant optical region, the size relationship for the static case remains valid for the dynamic $\gamma_{||}$ value that monotonically increases with an

increase of the applied field energies (Fig. 3). Similar to the α , the $\gamma_{||}$ values of the Si_2C and Si_3C clusters are smaller $\gamma_{||}$ than those of the Si_3 and Si_4 clusters, respectively, because the C atom with a static $\gamma_{||}$ value of 2194.32 a.u. (0.11×10^{-35} esu) [Ref. 51] is much smaller than the Si atom with that of 430000 a.u. (21.66×10^{-35} esu) [Ref. 3].

Table 3. Nine main components of the tensor γ and $\gamma_{||}^{\text{THG}}$ of the Si_2C and Si_3C clusters obtained using the CCSD/d-aug-cc-pVDZ response calculations. γ is expressed in 10^{-35} esu. $1 \text{ au} = 6.235 \times$

$$10^{-65} \text{ C}^4 \text{ m}^4 \text{ J}^3 = 5.036 \times 10^{-40} \text{ esu}$$

Cluster	γ_{xxxx}	γ_{yyyy}	γ_{zzzz}	γ_{xxyy}	γ_{xxzz}	γ_{yyzz}	γ_{yyxx}	γ_{zzxx}	γ_{zzyy}	$\gamma_{ }^{\text{THG}}$
$\hbar\omega = 0.0$ (eV)										
Si_2C	1.51	2.69	1.41	0.89	0.49	0.80	0.89	0.49	0.80	1.99
Si_3C	1.42	4.69	3.20	1.01	0.70	1.53	1.01	0.70	1.53	3.16
Si_3	2.69	5.53	3.13	1.26	1.00	1.75	1.26	1.00	1.75	3.87
Si_4	2.64	8.87	5.59	1.66	1.19	1.59	1.66	1.19	1.59	5.20
$\hbar\omega = 0.65$ (eV)										
Si_2C	1.80	3.23	1.66	1.10	0.58	0.99	0.89	0.57	0.95	2.40
Si_3C	2.08	5.68	3.78	2.08	1.00	1.95	1.25	0.84	1.84	4.10
Si_3	3.16	6.82	3.88	1.59	0.83	2.21	1.62	1.23	2.17	4.70
Si_4	2.71	10.78	6.83	0.88	1.36	1.88	2.27	1.48	1.85	6.01

3.4. $\gamma_{||}^{\text{THG}}$ of the Si_2C isomers

For the Si_3C cluster, experiments^{27, 52} and theoretical calculations^{29–31, 53} have consistently shown that the most stable structure (*i.e.*, ground state structure) is a rhomboidal structure with two equivalent silicon atoms and a trans-annular Si–C bond (Fig. 1). For the Si_2C cluster, however, two isomers (C_{2v} and $\text{D}_{\infty h}$ structures) were found with comparable energies^{28–31, 53–55}. A DFT study³¹ showed that these two isomers have a very close binding energy per atom (4.348 eV for C_{2v} and 4.346 eV for $\text{D}_{\infty h}$). More interestingly, for C_{2v} isomer, different theoretical calculations yielded different Si–C–Si bond angles (θ_{C}) within $114.5^\circ \sim 177.2^\circ$, while the experimental θ_{C} is 110° [Ref. 28 and 54]. Most theoretic bond lengths of Si–C (L_{C}) are 1.70 \AA while the experimental L_{C} is 1.75 \AA [Ref. 28 and 54]. At the B3LYP/aug-cc-pVTZ level, the isomer shown in Fig. 1 with a θ_{C} of 138.54° and a L_{C} of 1.694 \AA is a global minimum structure (see below).

Now let us investigate the θ_C by using PESS calculations. On the basis of previous theoretical and experimental researches on the geometries of the Si_2C cluster, PESS calculations were performed on C_{2v} symmetry structures at the B3LYP/aug-cc-pVTZ level, as implemented in the Gaussian 03 program³². In PESS calculations, two variables (θ_C and L_C) vary in the range of $110^\circ - 180^\circ$ with an increment-size of 5° and $1.64 - 1.94 \text{ \AA}$ with an increment-size of 0.02 \AA , respectively. The results are shown in Fig. 4 (left). Interestingly, for each θ_C , the lowest total energy lies at 1.70 \AA . For clarity, we give a plot of the total energy vs θ_C with a fixed L_C of 1.70 \AA in Fig. 4 (right). We can see from Fig. 4 (right) that structures of ten θ_C 's ($135, 140, 145, \dots, 180^\circ$ indicated by S135, S140, S145, ..., S180, respectively) have a very close total energy within an energy difference of ~ 0.00003 Hartree. Note that the PESS can only determine the approximate location of the minimum energy structure and does not perform geometry optimizations⁵⁶. Therefore, to identify stable structures, we run geometry optimizations for these ten structures and performed frequency analyses at the B3LYP/aug-cc-pVTZ level, as implemented in the Gaussian 03 program³². The vibrational frequencies ν and optimized θ_C and L_C for these ten structures are collected in Table 4. Four isomers (S150, S155, S160, and S165) lie at a saddle point because they have a negative frequency. And six isomers (S135, S140, S145, S170, S175, and S180) lie at a minimum point. S140 closes to the global minimum structure [Fig. 4 (left)]. In the following section, we focus on the $\gamma_{||}^{\text{THG}}$ of six minimum isomers.

Table 4. *Vibrational frequencies ν (cm^{-1}) and optimized θ_C ($^\circ$) and L_C (\AA) for ten structures*

	S135	S140	S145	S150	S155	S160	S165	S170	S175	S180
θ_C	135.05	139.96	144.94	149.94	154.95	159.98	165.00	170.01	175.09	180.0
L_C	1.695	1.695	1.694	1.694	1.694	1.694	1.694	1.694	1.694	1.694
ν	68.42	45.85	25.39	-11.49	-26.34	-32.05	-25.12	16.98	23.42	18.03 ^a
	740.07	713.48	687.15	661.92	639.15	619.69	603.83	591.93	584.40	582.02
	1316.07	1334.10	1349.75	1363.27	1374.79	1383.98	1390.94	1395.93	1398.72	1399.68

^a twofold degenerate

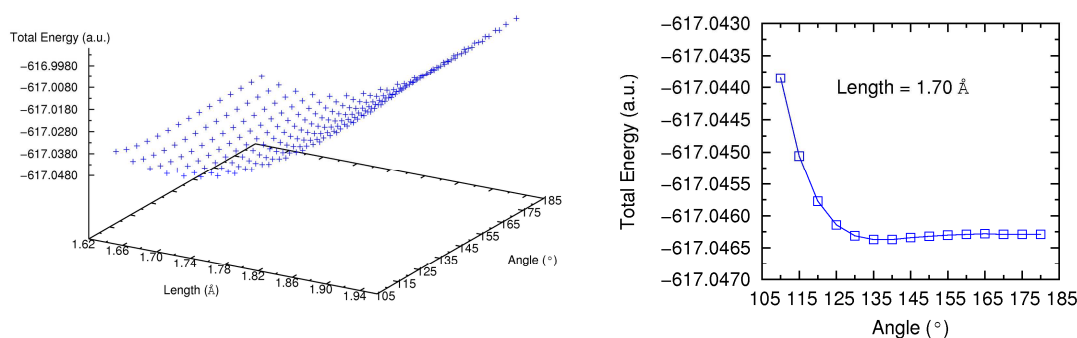


Figure 4. Total energy surface (left) and plot of the total energy vs θ_C with a fixed L_C of 1.70 Å (right) based on the B3LYP/aug-cc-pVTZ calculations.

The $\gamma_{||}^{\text{THG}}$ values of six minimum isomers for $\hbar\omega = 0.0$ and 0.65 eV are obtained using the CCSD/d-aug-cc-pVDZ response calculations. The results are shown in Table 5. In the static case, we find that the $\gamma_{||}^{\text{THG}}$ values increase slowly with an increase of the θ_C , and that the $\gamma_{||}^{\text{THG}}$ value of S180 is larger than that of S135 by 0.071×10^{-35} esu. For $\hbar\omega = 0.65$ eV, the same variable tendency as the static case is observed because the applied field energy of 0.65 eV lies in the non-resonant optical region, and the $\gamma_{||}^{\text{THG}}$ values at $\hbar\omega = 0.65$ eV have a difference of 0.131×10^{-35} esu between the S180 and S135 isomers. To obtain an in-depth understanding of non-resonance, in Table 5, we list the first ten excitation energies and the corresponding oscillator strengths of six minimum isomers obtained using the CCSD/d-aug-cc-pVDZ response calculations. From Table 5, we find that for six minimum isomers the first allowed transition has an excitation energy of ~ 3.39 eV and an oscillator strength of ~ 0.0355 (bold in Table 5). The possible resonance applied field energies are 3.39, 3.39 / 2, and 3.39 / 3 eV, which are far from 0.0 and 0.65 eV. Furthermore, the variable tendency of the $\gamma_{||}^{\text{THG}}$ value with the θ_C can be related to the change of frontier molecular orbitals. Figure 5 shows the HOMO and LUMO of six minimum isomers based on the B3LYP/aug-cc-pVTZ wave function. No change is observed for the LUMO, while a very clear change is for the HOMO. A change of the HOMO from σ -electron to π -electron framework results in a larger $\gamma_{||}^{\text{THG}}$ value of S170, S175, and S180 isomers than S135, S140, and S145 ones. This behavior is common for organic molecules, where molecules with π -electron framework, such as conjugate oligomers and polymers, have a larger (hyper)polarizabilities than ones with σ -electron framework, such as alkanes⁴¹. A change of HOMO is ultimately attributed to alternative sp^2 and sp hybridizations of the C atom.

Table 5. γ_{\parallel}^{THG} ($\times 10^{-35}$ esu) for $\hbar\omega = 0.0$ and 0.65 eV and the first ten excitation energies (eV) and the corresponding oscillator strengths (in parenthesis) of Si_2C isomers obtained using the CCSD/d-aug-cc-pVDZ response calculations. For γ_{\parallel}^{THG} , $1 \text{ au} = 6.235 \times 10^{-65} \text{ C}^4 \text{ m}^4 \text{ J}^3 = 5.036 \times 10^{-40} \text{ esu}$

	S135	S140	S145	S170	S175	S180
$\gamma_{\parallel}(0.0)$	1.978	1.996	2.011	2.047	2.048	2.049
$\gamma_{\parallel}(0.65)$	2.376	2.405	2.431	2.502	2.506	2.507
$E(f)$	3.24(0.0000)	3.17(0.0000)	3.11(0.0000)	2.95(0.0000)	2.93(0.0000)	2.93(0.0000)
	3.37(0.0014)	3.27(0.0008)	3.19(0.0004)	2.95(0.0000)	2.93(0.0000)	2.93(0.0000)
	3.42(0.0339)	3.40(0.0347)	3.32(0.0000)	2.99(0.0000)	2.97(0.0000)	2.96(0.0000)
	3.58(0.0000)	3.44(0.0000)	3.39(0.0355)	3.36(0.0382)	3.36(0.0383)	3.36(0.0384)
	3.80(0.0235)	3.70(0.0262)	3.62(0.0288)	3.38(0.0376)	3.36(0.0382)	3.36(0.0384)
	4.87(0.2327)	4.93(0.4326)	4.94(0.5969)	4.91(0.8682)	4.91(0.8838)	4.91(0.8889)
	4.95(0.0113)	5.07(0.0117)	5.18(0.0118)	5.52(0.0000)	5.51(0.0000)	5.51(0.0000)
	5.25(0.0051)	5.33(0.0058)	5.41(0.0061)	5.54(0.0096)	5.52(0.0025)	5.51(0.0000)
	5.33(0.5605)	5.38(0.3736)	5.47(0.2215)	5.60(0.0036)	5.63(0.0008)	5.64(0.0000)
	5.67(0.0017)	5.67(0.0011)	5.64(0.0000)	5.66(0.0016)	5.68(0.0004)	5.69(0.0000)

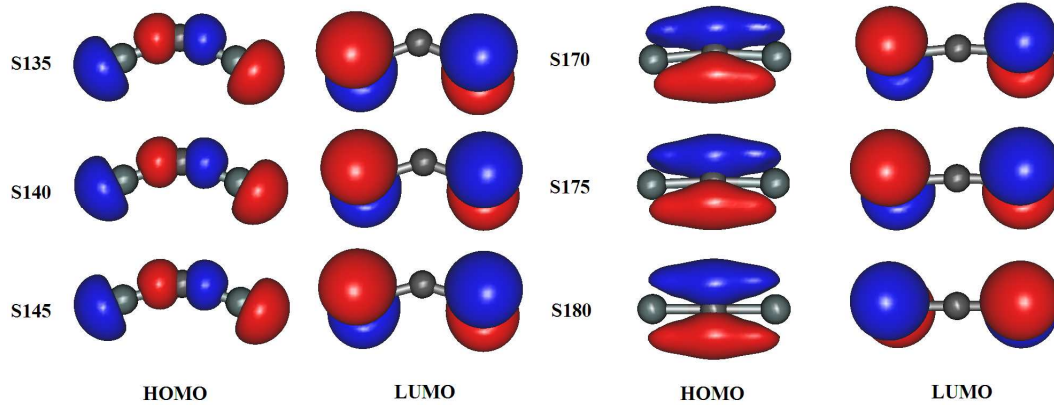


Figure 5. HOMO and LUMO of the Si_2C isomers based on the B3LYP/aug-cc-pVTZ wave function.

4. Conclusions

We have investigated the dynamic γ_{\parallel}^{THG} of the Si_2C and Si_3C clusters using highly accurate

CCSD response approach. On the basis of Paterson *et al.*'s work⁴² and our present results, we suggest that the reliable results should be obtained for the optical properties related to cubic response function using the CCSD with the doubly and the triply augmented double- or triple-zeta Dunning basis sets response calculations. The dynamic $\gamma_{||}^{\text{THG}}$ of the Si₂C and Si₃C clusters, as well as the Si₃ and Si₄ clusters¹⁴, exhibit wide non-resonant optical region because there are long absorption tails in their linear absorption spectra. In the non-resonant optical region, similar to the α values, the γ values of the Si₂C and Si₃ clusters are individually smaller than those of the Si₃ and Si₄ clusters. These clusters are expected to be potential candidates for third-order nonlinear optical materials in the infrared region.

The C_{2v} Si₂C isomers have been searched by using PESS calculations. We focus on ten possible isomers including the D_{∞h} isomer. Frequency analyses showed that four of them lie at a saddle point and six of them lie at a local minimum point. We have calculated the $\gamma_{||}^{\text{THG}}$ values of six minimum isomers for $\hbar\omega = 0.0$ and 0.65 eV using the CCSD/d-aug-cc-pVDZ response calculations. The $\gamma_{||}^{\text{THG}}$ values of these six isomers exhibit a monotonically increasing angle-dependence, which can be related to a change of HOMO from σ -electron to π -electron framework. It should be noted that for the Si₃ cluster, it has two spin states (C_{2v} singlet and D_{3h} triplet) with very close energy^{11,57}, while their relative stabilities depend on level of theory. These two spin states have fairly different theoretical α values¹¹. Therefore, what about their hyperpolarizabilities? And what is the influence of spin state on the hyperpolarizabilities? The PESS calculation for the Si₃ cluster would also be necessary. This work is in progress.

Acknowledgements

We appreciate the financial support from the Foundation of Zhejiang Key Laboratory for Reactive Chemistry on Solid Surfaces.

References

- ¹ I. Vasiliev, S. Ögüt and J. R. Chelikowsky, Phys. Rev. Lett. **78**, 4805 (1997).
- ² V. E. Bazterra, M. C. Caputo, M. B. Ferraro and P. Fuentealba, J. Chem. Phys. **117**, 11158 (2002).
- ³ G. Maroulis and C. Pouchan, J. Phys. B: At. Mol. Opt. Phys. **36**, 2011 (2003).

- ⁴ K. A. Jackson, M. Yang, I. Chaudhuri and Th. Frauenheim, Phys. Rev. A **71**,033205 (2005).
- ⁵ Y. Mochizuki and H. Ågren, Chem. Phys. Lett. **336**, 451 (2001).
- ⁶ K. Deng, J. L. Yang, and C. T. Chan, Phys. Rev. A, **61**, 025201 (2000)
- ⁷ K. Jackson, M. Pederson, C. Z. Wang, and K. M. Ho, Phys. Rev. A **59**, 3685 (1999).
- ⁸ C. Pouchan, D. Bégué and D. Y. Zhang, J. Chem. Phys. **121**, 4628 (2004).
- ⁹ G. Maroulis, D. Bégué and C. Pouchan, J. Chem. Phys. **119**, 794 (2003).
- ¹⁰ G. Maroulis and C. Pouchan, Phys. Chem. Chem. Phys. **5**, 1992 (2003).
- ¹¹ D. Bégué, C. Pouchan, G. Maroulis, and D. Y. Zhang, J. Comp. Meth. Sci. Eng. **6**, 223 (2006).
- ¹² R. Schäfer, S. Schlecht, J. Woenckhaus, and J. A. Becker, Phys. Rev. Lett. **76**, 471 (1996).
- ¹³ T. T. Rantala and M. I. Stockman, D. A. Jelski, and T. F. George, J. Chem. Phys. **93**, 7427 (1990).
- ¹⁴ Y. Z. Lan, Y. L. Feng, Y. H. Wen, and B. T. Teng, Chem. Phys. Lett. **461**, 118 (2008).
- ¹⁵ Y. Z. Lan and Y. L. Feng, J. Chem. Phys. **131**, 054509 (2009).
- ¹⁶ Y. Z. Lan, Y. L. Feng, Y. H. Wen and B. T. Teng, J. Mol. Struct. (Theochem) **854**, 63 (2008).
- ¹⁷ Y. Z. Lan, W. D. Cheng, D. S. Wu, J. Shen, S. P. Huang, H. Zhang, Y. J. Gong and F. F. Li, J. Chem. Phys. **124**, 094302 (2006).
- ¹⁸ Y. Z. Lan, W. D. Cheng, D. S. Wu, X. D. Li, H. Zhang and Y. J. Gong, Chem. Phys. Lett. **372**, 645 (2003).
- ¹⁹ P. P. Korambath and S. P. Karna, J. Phys. Chem. A **104**, 4801 (2000)
- ²⁰ B. Champagne, M. Guillaume, D. Bégué, and C. Pouchan, J. Comp. Meth. Sci. Eng. **7**, 297 (2007)
- ²¹ A. Sieck, D. Porezag, Th. Frauenheim, M. R. Pederson and K. Jackson, Phys. Rev. A, **56**, 4890 (1997).
- ²² H.S. Nalwa, *Handbook of Thin Films Materials*, Volume 5: Nanomaterials and Magnetic Thin Films. Academic Press, New York, and 2002, Chapter 2
- ²³ P. Karamanis, D. Bégué, and C. Pouchan, J. Chem. Phys. **127**, 094706 (2007).
- ²⁴ S. Vijayalakshmi, M. A. George, and H. Grebel, Appl. Phys. Lett. **70**, 708 (1997).
- ²⁵ S. Vijayalakshmi, F. Shen, and H. Grebel, Appl. Phys. Lett. **71**, 3332 (1997).
- ²⁶ R. Orlando, M. Ferrero, M. Rérat, B. Kirtman, and R. Dovesi, J. Chem. Phys. **131**, 184105 (2009)

- ²⁷ J. D. Presilla-Márquez and W. R. M. Graham, *J. Chem. Phys.* **96**, 6509 (1992).
- ²⁸ Z. H. Kafafi, R. H. Hauge, L. Fredin, and J. L. Margrave, *J. Phys. Chem.* **87**, 797 (1983).
- ²⁹ M. Bertolus, V. Brenner, and P. Millié, *Eur. Phys. J. D* **1**, 197 (1998).
- ³⁰ J. L. Deng, K. H. Su, X. Wang, Q. F. Zeng, L. F. Cheng, Y. D. Xu, and L. T. Zhang, *Eur. Phys. J. D* **49**, 21 (2008) and references therein.
- ³¹ P. Pradhan and A. K. Ray, *J. Mol. Struct.(THEOCHEM)* **716**, 109 (2005).
- ³² M. J. Frisch, G. W. Trucks, H. B. Schlegel *et al.*, Gaussian 03, Revision D.01, Gaussian, Inc., Wallingford, CT, **2004**.
- ³³ DALTON, a molecular electronic structure program, Release 2.0 (2005), see <http://www.kjemi.uio.no/software/dalton/dalton.html>.
- ³⁴ J. Olsen and P. Jørgensen, *J. Chem. Phys.* **82**, 3235 (1985).
- ³⁵ O. Christiansen, A. Halkier, H. Koch, P. Jørgensen, and T. Helgaker, *J. Chem. Phys.*, **108**, 2801 (1998).
- ³⁶ C. Hättig, O. Christiansen, H. Koch, and P. Jørgensen, *Chem. Phys. Lett.* **269**, 428 (1997).
- ³⁷ C. Hättig, O. Christiansen, and P. Jørgensen, *Chem. Phys. Lett.* **282**, 139 (1998).
- ³⁸ P. Salek, O. Vahtras, T. Helgaker, and H. Ågren, *J. Chem. Phys.* **117**, 9630 (2002).
- ³⁹ B. Jansik, P. Salek, D. Jonsson, O. Vahtras, and H. Ågren, *J. Chem. Phys.* **122**, 054107 (2005).
- ⁴⁰ D. P. Shelton and J. E. Rice, *Chem. Rev.* **94**, 3 (1994).
- ⁴¹ J. L. Brédas, C. Adant, P. Tackx, A. Persoons, and B. M. Pierce, *Chem. Rev.* **94**, 243 (1994).
- ⁴² M. J. Paterson, O. Christiansen, F. Pawłowski, P. Jørgensen, C. Hättig, T. Helgaker, and P. Salek, *J. Chem. Phys.* **124**, 054322 (2006).
- ⁴³ C. Hättig, O. Christiansen, and P. Jørgensen, *J. Chem. Phys.* **108**, 8355 (1998).
- ⁴⁴ B. Jansik, P. Salek, D. Jonsson, O. Vahtras, and H. Ågren, *J. Chem. Phys.* **122**, 054107 (2005).
- ⁴⁵ C. Hättig, O. Christiansen, and P. Jørgensen, **108**, 8331 (1998).
- ⁴⁶ A.R. Allouche, Gabedit is a free Graphical User Interface for computational chemistry packages. It is available from <http://gabedit.sourceforge.net/>
- ⁴⁷ I. Vasiliev, S. Ögüt and J. R. Chelikowsky, *Phys. Rev. B.* **60**, R8477 (1999).
- ⁴⁸ H. Koch, O. Christiansen, P. Jørgensen, and J. Olsen, *Chem. Phys. Lett.* **244**, 75 (1995)
- ⁴⁹ O. Christiansen, H. Koch, P. Jørgensen, and J. Olsen, *Chem. Phys. Lett.* **256**, 185 (1996)
- ⁵⁰ P. Fuentealba, *Phys. Rev. A*, **58**, 4232 (1998)

- ⁵¹ L. Jensen, K. O. Sylvester-Hvid, K. V. Mikkelsen, and P. Åstrand, *J. Phys. Chem. A*, **107**, 2270 (2003).
- ⁵² J. F. Stanton, J. Dudek, P. Theulé, H. Gupta, M. C. McCarthy, and P. Thaddeus, *J. Chem. Phys.* **122**, 124314 (2005).
- ⁵³ Z. Y. Jiang, X. H. Xu, H. S. Wu, F. Q. Zhang, Z. H. Jin, *J. Mol. Struct.(THEOCHEM)* **621**, 279 (2003).
- ⁵⁴ J. D. Presilla-Márquez and W. R. M. Graham, *J. Chem. Phys.* **95**, 5612 (1991).
- ⁵⁵ R. S. Grev and H. F. Schaefer III, *J. Chem. Phys.* **82**, 4126 (1985)
- ⁵⁶ J. B. Foresman and Æ. Frisch, *Exploring Chemistry with Electronic Structure Methods*, 2nd ed. (Gaussian, Inc., Pittsburgh, PA, 1996).
- ⁵⁷ R. S. Grev and H. F. Schaefer, *Chem. Phys. Lett.* **119**, 111 (1985).